Journal of Radioanalytical and Nuclear Chemistry (2021) 327:869–875
https://doi.org/10.1007/s10967-020-07546-2

# Separation of astatine from irradiated lead targets based on dry distillation in a glass test tube

**Ichiro Nishinaka**[1] · **Kazuyuki Hashimoto**[1]

Received: 13 September 2020 / Accepted: 5 December 2020 / Published online: 25 January 2021


**Abstract**
Astatine was separated from a lead target, irradiated with $^{7}$Li ion beams, by dry distillation. Dry distillation was conducted in a glass test tube filled with nitrogen gas by heating the test tube with an electric furnace at 650 °C. The optimized conditions of the dry distillation procedure were studied by monitoring astatine radioactivity with gamma-ray spectrometers. The separation of astatine was accomplished in ~ 10 min. The cooling of the middle portion of the test tube was instrumental in recovering astatine radioactivity in high yields. The adsorption temperature of astatine on the glass surface was ~ 20 °C.

**Keywords** Astatine · Separation · Dry distillation · Optimized conditions · Lead target · Adsorption temperature

## Introduction

In general, the $^{211}$At radionuclide, which is a prospective candidate for utilization in targeted alpha therapy, is produced through the $^{209}$Bi($^{4}$He, 2n)$^{211}$At reaction [1–11]. The isolation of $^{211}$At from an irradiated bismuth target was employed by dry-distillation, using specific apparatuses [1–4, 6, 8, 11]. Such isolation methods focused on the preparation of astatine with its high yields required for therapeutic purposes.

Complementary and unique production routes of astatine have been recently obtained by $^{7}$Li ion beams [12–14]. The lithium induced reaction on natural lead target, $^{nat}$Pb($^{7}$Li, xn)$^{207–211}$At, provided gamma emitters of astatine. One of the gamma-emitting radionuclides, $^{210}$At ($T_{1/2}$ = 8.1 h), is unsuitable for medical use because $^{210}$At decays via EC/$\beta^{+}$, with 99.8% probability, to the highly radiotoxic alpha emitter, $^{210}$Po. In contrast, $^{210}$At is suitable for fundamental studies owing to the convenience of gamma-ray detection, i.e., transmittivity and quantitativeness. To use astatine radionuclides produced in the $^{nat}$Pb($^{7}$Li, xn)$^{207–211}$At reactions, we developed a procedure for the preparation of no-carrier-added astatine tracer solutions. The procedure was simply and readily conducted without specific apparatuses in a conventional laboratory [14]. This has recently enabled and confirmed the speciation of astatine chemical species, astatide ($At^{-}$), astatate ($AtO_3^{-}$), and perastatate ($AtO_4^{-}$), by thin layer chromatography on silica gel with an ethanol-water solution [15, 16]. Of note, the understanding of basic chemical and radiochemical properties of astatine is still challenging [17].

The preparation of astatine tracer solutions was performed in a glass test tube in two steps, i.e., (1) the separation of astatine from the melted lead target by dry distillation, and (2) the elution of separated astatine with a solution. The second step for elution has been reported in some details [14–16]. Here, we aim to study optimized conditions of dry distillation in the first step. The conditions of dry distillation were investigated by measuring the radioactivity of astatine radionuclides with two lead-shielded gamma-ray spectrometers (GRSs). GRSs demonstrated the time dependence of dry distillation and the distribution of astatine radioactivity in the test tube after dry distillation. The results were compared with those in the general production through the $^{209}$Bi($^{4}$He, 2n)$^{211}$At reaction, which was conducted with the almost identical experimental setup optimized on the basis of the present study [18]. Finally, the adsorption temperature ($T_{ads}$) of astatine was compared with the reported data [18–20] owing to the fundamental interest of volatile astatine species.

✉ Ichiro Nishinaka
nishinaka.ichiro@qst.go.jp

[1] Tokai Quantum Beam Science Center, Takasaki Advanced Radiation Research Institute, National Institutes for Quantum and Radiological Science and Technology, Shirakata-Shirane 2-4, Tokai-mura, Naka-gun, Ibaraki 319-1106, Japan

## Experimental

### Production of astatine radionuclides

Lead targets with the thickness of approximately 1 mg $cm^{-2}$ were prepared by vacuum evaporation onto a foil backing of 5.4 mg $cm^{-2}$ aluminum. Each target was covered with another 5.4 mg $cm^{-2}$ aluminum foil, and produced astatine radionuclides, which recoiled out from lead targets, were collected. A stack of targets, which was placed in a water-cooled Faraday cup, was irradiated with 60 MeV $^{7}Li^{3+}$ ions, supplied from the Japan Atomic Energy Agency (JAEA) tandem accelerator. The beam current of 80–200 nA was employed during the irradiation for 0.5–2.0 h. After irradiation, the amount of astatine radionuclides $^{209,210}$At was determined with a Ge detector by gamma-ray spectrometry. The details of the production and gamma-ray spectrometry were reported in Ref. [14, 15].

### Dry distillation

The separation of astatine from irradiated lead was conducted with an experimental setup for dry distillation, as schematically shown in Fig. 1. Dry distillation was performed in a glass test tube (length 180 mm; inner diameter 16 mm) with an electric furnace, as described in Ref. [14]. However, two cadmium–zinc–tellurium (CZT) GRSs (GR-1, Kromek) were introduced to study the heating time required to separate astatine from the irradiated lead target, as has been previously reported in Ref. [18]. The experimental setup in Ref. [18] was almost identical with the present one (Fig. 1) but was optimized to monitor at the distance of 10 cm on the basis of the present study. CZT GRSs, connected to a personal computer through USB cables, were individually placed in a shielding stainless steel container (thickness 3 mm) that was filled with lead metal (~25 mm thickness). The shielding had a 16 × 16 mm window, through which CZT GRSs measureed gamma-rays. CZT GRSs, which were placed in the shielding, monitored radioactivities during heating in dry distillation as well as radioactivity distributions in the test tubes after dry distillation.

The test tube holding the irradiated target was filled with nitrogen gas and doubly sealed with a polyethylene film (DureSeal™, Diversified Biotech). A portion of the test tube, in the region of 10–14 cm from the bottom, was cooled to approximately − 5 °C with a thermoelectric cooler (OCE-F15P-D12, OHM Electric Co. Ltd.). Figure 2 shows the experimental setup just before mounting the electric furnace on the test tube. The target was heated for 15 min, at 650 °C, with the electric furnace, by mounting on the third portion of the bottom of the test tube. Spectra, measured by GRSs, were sequentially recorded at 60 s intervals with the USB multichannel analyzer software (MultiSpect Analysis, Kromek), which was installed on a personal computer, to monitor the time dependence of dry distillation.

After demounting the electric furnace, the test tube was cooled to ambient temperature (~23 °C) for 10 min in air; then, it was demounted from the thermoelectric cooler. After opening the test tube and removing the target from it, the relative intensities of astatine radioactivity, separated and adsorbed on the inner wall of the test tubes, were measured across the length in 2 cm steps with CZT GRS, collimated with shielding, to study the astatine distribution after dry distillation. In addition, the amounts of astatine radioactivity, which were maintained in the target and attached to the polyethylene firm applied to the test tube opening, were individually measured with the Ge detector.

Dry distillation trials were also employed without using the thermoelectric cooler, as shown in Fig. 3. The test tube holding the target was placed into the electric furnace at 650 °C while vertically tilted to heat for 15 min. The relative

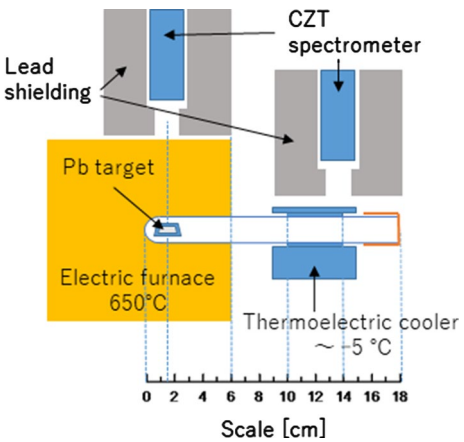


**Fig. 1** Experimental setup for dry distillation

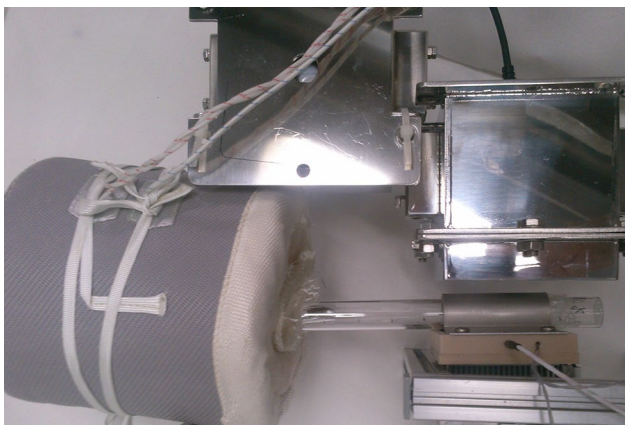

**Fig. 2** Top view of the experimental setup for dry distillation

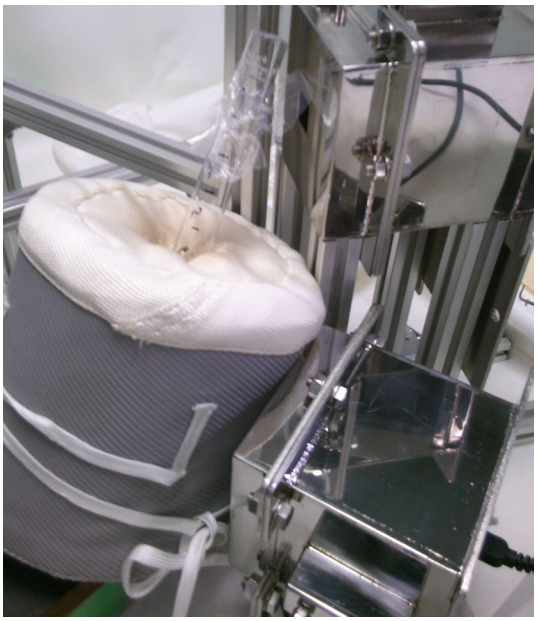

**Fig. 3** Side view of the experimental setup without using a thermoelectric cooler for dry distillation

amounts of radioactivity were simultaneously measured both at the target portion and the portion near the test tube opening to study the time dependence of dry distillation. The measurements of astatine radioactivity after dry distillation were conducted using the aforementioned approach.

In the experiments without using radioactivity, the temperatures of the outer wall of the test tube were measured with two thermocouples (Ultra Fine Temperature Sencer, AS ONE Corp.) under the same conditions as those in the experiments employing radioactivity to obtain astatine distribution in the test tube. The data were recorded at 10 s intervals for ~ 10 min with two instruments (K Thermocouple Data Logger, RX-450K, AS ONE Corp.) that were individually connected to the thermocouples.

## Results and discussion

### Dry distillation with cooling

The typical gamma spectra of astatine, separated by dry distillation, are shown in Fig. 4 and were measured with CZT (thick line) and Ge (thin line) detectors. The measurement samples were the test tube and the polyethylene film for CZT and Ge, respectively, which were prepared during a dry distillation trail with cooling. During the trial, the amounts of radioactivity in the lead target were 90 and 31 kBq for $^{210}$At and $^{209}$At, respectively. The number of astatine atoms used was ~ $7 \times 10^9$, including $^{211}$At, and was estimated from the production cross sections [14]. These astatine nuclides

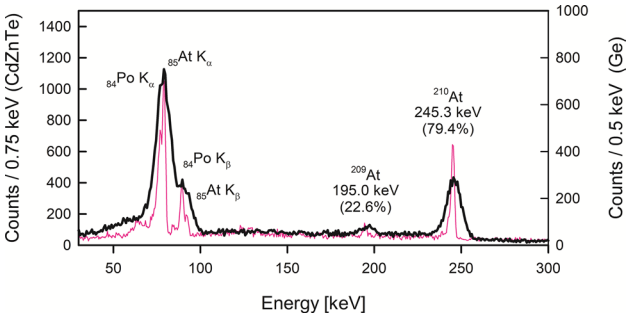


**Fig. 4** Gamma spectra of astatine radionuclides, measured for 300 s with the CZT gamma-ray spectrometer (thick line) and for 2454 s with a Ge detector (thin line) after 21 h of EOB

were produced in the 49 MeV $^7$Li + $^{nat}$Pb reaction and were utilized 18 h after the end of bombardment (EOB). Of note, photopeaks of only astatine were observed, which indicated that separation was successfully performed with high purity.

As shown in Fig. 4, the CZT detector has low efficiency for high-energy gamma-ray and low energy resolution compared with the Ge detector. Therefore, the characteristic X-rays of astatine and polonium at approximately 80 and 90 keV for $K_\alpha$ and $K_\beta$, respectively, were used to obtain the relative intensities of astatine radioactivity by summing up counts in the region of 55–100 keV of each gamma spectrum, which exhibit the heating time dependence and distribution in the test tubes of astatine activities. In contrast, the intensities of photopeak at 235.4 keV for $^{210}$At in the spectra measured with the Ge detector, with subtracted backgrounds, were utilized to quantitate the amount of astatine radioactivity that was produced in the target, maintained in the target, and attached to the polyethylene film after dry distillation.

The relative intensities are shown as functions of heating time in Fig. 5. The intensities at the target portion (open circle) greatly dereased from 4 to 10 min, whereas those at the test tube portion (closed circle) greatly increased. This behavior clearly indicates the dry distillation process. Specifically, the lead metal target conducted heat and melted in ~ 4 min, and then astatine escaped from melted lead and rapidly transported to the test tube opening in ~ 10 min. Compared with the production through the $^{209}$Bi($^4$He, 2n)$^{211}$At reaction [18], the data, obtained from Ref. [18], are displayed as dashed and dash-dotted lines in Fig. 5 and normalized to the current data. It is remarkable that dry distillation was quickly accomplished for the target produced in $^{209}$Bi($^4$He, 2n)$^{211}$At (~ 6 min) compared with that produced in the $^{nat}$Pb($^7$Li, xn)$^{207–211}$At reaction (~ 10 min). This is reasonably related to the physical properties of metal targets, bismuth and lead; melting point, 272 °C and 327 °C; thermal conductivity, 7.97 and 35.3 W m$^{-1}$ K$^{-1}$ at 300 K, respectively.

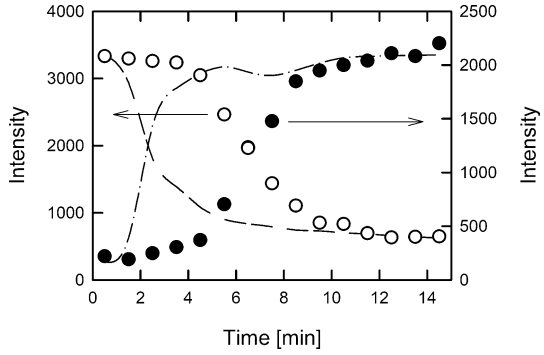


**Fig. 5** Dependence of astatine radioactivity on heating time at the target portion (open circle and dashed line) and the portion near the test tube opening (solid circle and dash-dotted line) in the dry distillation trial with the electric cooler; $^{nat}$Pb($^{7}$Li, xn)$^{209–211}$At in this work (open and solid circles) and $^{209}$Bi($^{4}$He, 2n)$^{211}$At obtained from Ref. [18] (dashed and dash-dotted lines)

Astatine, which was separated from the lead target by dry distillation, was widely distributed across the length of the test tube, as shown by closed circles and solid line in Fig. 6. (Dashed line indicates data for $^{209}$Bi($^{4}$He, 2n)$^{211}$At obtained from Ref. [18]. This will be discussed in details later.) However, large amounts of astatine were deposited in the middle portion of the test tube. This was determined from the amounts of radioactivity in the target before and after dry distillation and on the polyethylene firm, measured with the Ge detector, as listed in Table 1, normalized as the radioactivity in lead target before dry distillation became 100%. The errors in the relative amounts, not shown in Table 1, were ~4% for each value and estimated from the ambiguity of gamma-ray spectrometry. Of note, dry distillation with cooling rapidly and successfully separated astatine from the melted lead target with the high yield of ~93% but

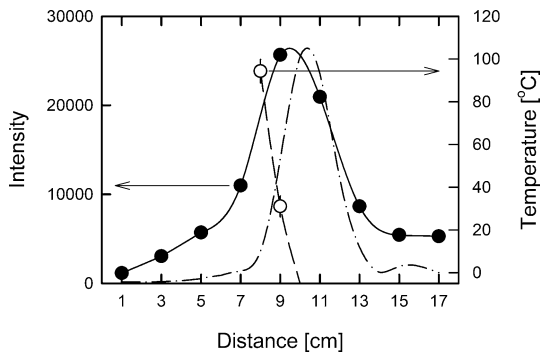


**Fig. 6** Distribution of astatine radioactivity (closed circle and solid and dash-dotted lines) and temperatures (open circle and dashed line) across the length as functions of distance from the bottom of the test tube in the dry distillation trial with the electric cooler; $^{nat}$Pb($^{7}$Li, xn)$^{209–211}$At in this work (open and solid circles and solid and dashed lines) and $^{209}$Bi($^{4}$He, 2n)$^{211}$At obtained from Ref. [18] (dash-dotted line)

**Table 1** Distribution of astatine activity in the test tube after dry distillation

| Dry distillation trials | Relative amounts (%) | | |
|---|---|---|---|
| | In the target | On the polyethylene film | On the test tube wall |
| Trial with cooling | 4.3[a] | 3.1[a] | 92.6[b] |
| Trial without cooling | 4.5[a] | 16.7[a] | 78.8[b] |

[a]Measured with a Ge detector

[b]Calculated from the measured values in target and on polyethylene film

maintained radioactive impurities in it. In contrast, rather small amounts were maintained in the target (~4%), and adsorbed on the polyethylene film (~3%).

In Fig. 6, the temperatures of test tube, measured with the thermocouples, are also shown as open circles and dashed line in the 8–10 cm region. The bottom of the test tube was heated to 650 °C in an electric furnace, whereas the 10–14 cm portion was cooled to approximately −5 °C. This provided a large temperature gradient from 650 °C to approximately −5 °C in the range of 3–10 cm of the test tube. The measured temperatures were 94 ± 6 °C and 31 ± 5 °C at 8 and 9 cm, respectively, on the outer wall of the test tube. The temperatures and errors refer to the average and standard deviation, respectively, obtained from the data, recorded at 10 s intervals, for 8 min out of ~10 min, with two thermocouples. Thus, the $T_{ads}$ of astatine on glass was estimated at ~20 °C, from the temperature at the peak of the astatine radioactivity distribution in Fig. 6. $T_{ads}$ will be discussed in details later.

## Dry distillation without cooling

The results of dry distillation without using the thermoelectric cooler are shown in Figs. 7 and 8. The amounts of astatine radioactivity in the lead target at the dry distillation trial were 217 and 139 kBq for $^{210}$At and $^{209}$At, respectively. The number of astatine atoms used was ~$2 \times 10^{10}$, including $^{211}$At, estimated from the production cross sections [14]. These astatine nuclides were produced during the 46 MeV $^{7}$Li + $^{nat}$Pb reaction and were utilized after 9 h of EOB.

The heating time dependence of dry distillation, as shown in Fig. 7, is identical to that shown in Fig. 5. Dry distillation started in ~4 min, and ended in ~10 min. Such similarity is because cooling results in adsorption compared with dry distillation. After 10 min of heating, large relative intensities seem to remain in the target compared with those in Fig. 5. However, the amount of astatine remained in the target, determined with the Ge detector, was comparable in both experiments, as shown in Table 1. It was determined that

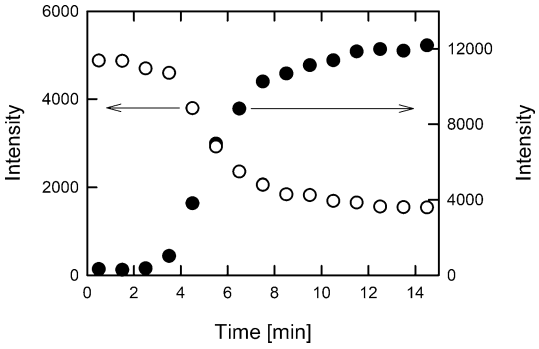


**Fig. 7** Dependence of astatine activities on heating time at the target portion (open circle) and the portion near the test tube opening (solid circle) in the dry distillation trial without an electric cooler

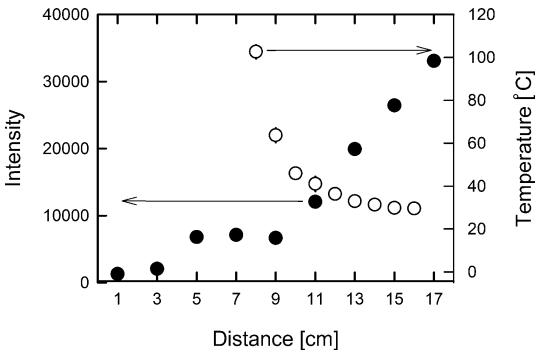


**Fig. 8** Distribution of astatine activity (closed circle) and temperatures (open curcle) measured across the length as a function of distance from the bottom of the test tube in the dry distillation trial without the electric cooler

considerable amounts of relative intensities, measured with CZT GRS, at the target after distillation, originated from the radioactivities of polonium and other elements, produced in the reactions of lead and elements in the aluminum foil backing with lithium beams.

However, the distribution of astatine radioactivity and temperatures represent rather different profiles in the dry distillation trial without cooling (closed circle in Fig. 8), compared with those with cooling (Fig. 6). Although some astatine was adsorbed on the inner wall of the test tube in the region from 5 to 9 cm near the opening of the electric furnace (~7 cm), the intensities increased with distance, which indicated that large quantities of separated astatine traveled to the test tube opening without adsorbing on the test tube. In addition, this resulted in the large relative amount of 16.7% on the polyetylene film applied to the test tube opening, compared with 3.1% for the trial with cooling, as shown in Table 1.

Such adsorption behavior is reasonably related to the temperature profile, as indicated by open circles in Fig. 8. The test tube exhibited a large temperature gradient at the distance < 10 cm owing to its low heat conductivity, which is similar to that shown in Fig. 6. At the distance > 10 cm, the temparature gradually decreased and approached ambient temperature (~23 °C) and remained greatger than the $T_{ads}$ of 20 °C, as determined from the observation in Fig. 6. This result suggested that during the trial without cooling, separated astatine traveled to the test tube opening, and then it was moderately adsorbed and/or deposited on the inner wall of the test tube.

Of note, even during the trial without cooling, the substantially high yield of ~79% can be effortlessly and successfully obtained with high purity, by the dry distillation method, as listed in Table 1. However, the yield is clearly small compared with ~93% with cooling. Of note, cooling the middle portion of the test tube was instrumental in recovering the astatine activity in high yield.

## Adsorption temperature of astatine

In previous studies [14–16, 18], volatile astatine has been considered to form $At^0$ because it escaped from melted lead into nitrogen gas, and the existence of molecular astatine was excluded by its low concentration in the order of ~$10^{10}$ [14–16] and ~$10^{12}$ [18] atoms ($^{209–211}$At). However, the present results suggest the reconsideration of $T_{ads}$ and volatile chemical species of astatine by comparing the previously reported studies [18–20].

The $T_{ads}$ of ~20 °C, determined in this study, was comparable with that of 16 °C for $At_2$, reported by Merinis et al. [19]. The reported temperature of 16 °C was measured in the experiment using the quartz tube (length: 100 cm, inner diameter 0.2 cm) with a thermal gradient from 500 °C to > − 130 °C, employing helium gas at the flow rate of 0.1 mL $s^{-1}$. The species $At_2$ ($10^{8–9}$) was assigned by comparing the depositions of AtCl ($10^{8–9}$) at 100 °C, AtBr ($10^{8–9}$) at 70 °C, and AtI ($10^{8–9}$) at 35 °C, where the amounts of radioactive astatine atoms, $^{209–211}$At, utilized in the experiments, are indicated in parentheses. In addition, the assignments of astatine species were supported by comparing the deposition of ICl ($10^{10}$) at 46 °C, IBr ($10^{10}$) at 14 °C, $I_2$ ($10^{15}$) at − 5 °C, I ($10^{9–10}$) at 200 °C and BrCl ($10^{15}$) at − 32 °C. Such interhalogene compounds of radioactive astatine ($^{209–211}$At), iodine ($^{131}$I), and bromine ($^{82}$Br) were synthesized with the flowing gas, chlorine, a mixture of helium and bromine, or a mixture of helium and iodine under similar experimental conditions instead of helium. Of note, for iodine, using helium gas, the concentration dependence of deposition was reported: the atomic state, I, deposited at 200 °C in low amount, was on the order of $10^9$–$10^{10}$ atoms, whereas the molecular state, $I_2$, was deposited at − 5 °C in a slightly higher amount, i.e., on the order of $10^{15}$ atoms. In addition, the high temperature deposition of atomic form, At, unlike iodine, was not

observed even at low concentration on the order of $10^8$–$10^9$ atoms. These observations implied that astatine formed the molecular state at lower concentration than iodine [19].

Whereas, the high $T_{ads}$s of 272 °C for At and 73 °C for $AtO_2$ on the quartz surface have been reported by Serov et al. [20]. The reported $T_{ads}$s were measured when using the quartz tube (length, ~ 56 cm; inner diameter, 4 mm) with a thermal gradient from ~ 1000 to approximately − 196 °C. The measurements were conducted by flowing a carrier gas: 272 °C and 73 °C were obtained, employing pure hydrogen and pure oxygen (or $O_2$/$H_2O$) gas, respectively, at the flow rate of 15 mL $min^{-1}$. The amounts of astatine atoms utilized in Ref. [20] were unknown but expected to be much smaller than that in Ref. [19] and $At_2$ was not observed.

Of note, it is cleart that $T_{ads}$s of ~ 20 °C on glass and 16 °C on quartz, observed in this study and Ref. [19], respectively, largely deviate from 272 °C and 73 °C on quartz in Ref. [20]. This suggests that astatine on the order of $10^8$–$10^{10}$ atoms could form species, such as $At_2$, in inactive gases, i.e., nitrogen and helium. Owing to such relation between $T_{ads}$s and concentrations of astatine used, the astatine distribution shown in Fig. 6 was reconsidered by comparing that for $^{nat}$Pb($^7$Li, xn)$^{209–211}$At (solid circles and line) in this study with that for $^{209}$Bi($^4$He, 2n)$^{211}$At (dash-dotted line) in Ref. [18], using an almost identical experimental setup.

The data obtained from Ref. [18] and normalized to these data exhibit large and small components at ~ 10.5 and ~ 15.5 cm, respectively. (The small component at ~ 15.5 cm was formed by deposition on a silicon plug, used to prevent the leakage of astatine.) The large component at ~ 10.5 cm overlapped but was located at large distance with a small width compared with the peak for $^{nat}$Pb($^7$Li, xn)$^{209–211}$At (solid circles and line). The difference in deposition was related to astatine amounts on the order of ~ $10^{12}$ and ~ $10^{10}$ atoms for $^{209}$Bi($^4$He, 2n)$^{211}$At and $^{nat}$Pb($^7$Li, xn)$^{209–211}$At, respectively. Specifically, the molecular state, $At_2$, can deposit at a slightly higher amount (~ $10^{12}$) for $^{209}$Bi($^4$He, 2n)$^{211}$At, whereas both molecular and atomic states, $At_2$ and At, could deposit at a low amount (~ $10^{10}$) for $^{nat}$Pb($^7$Li, xn)$^{209–211}$At. For $^{nat}$Pb($^7$Li, xn)$^{209–211}$At shown in Figs. 6 and 8, the atomic state, At, at $T_{ads}$s = 272 °C, can be observed as deposition at the distance of 5–9 cm near the opening of the electric furnace (~ 7 cm). Unfortunately, the current experimental setup cannot differentiate between of $At_2$ and At deposition owing to the large temperature gradient at short distance. However, the comparison of observations assumed that $T_{ads}$ = ~ 20 °C, preliminarily determined from Fig. 6, was not for $At_2$ but for the mixture of $At_2$ and At.

Finally, for such assumption based on volatile chemical species of astatine, the $T_{ads}$ for $At_2$ was revalidated at approximately − 10 °C from Fig. 6 and the setting temperature of the thermoelectric cooler in Ref. [18], although the temperature ~ 20 °C, estimated from the measurement at the distance of 9 cm, was preliminarily assigned as $T_{ads}$ in Ref. [18]. The $T_{ads}$ of approximately − 10 °C revalidated for $At_2$ (~ $10^{12}$) is low compared with that of 16 °C for $At_2$ ($10^{8–9}$) in Ref. [19]. This probably originated from the current experimental setup. In this present study and in Ref. [18], the experimental setup with large temperature gradient and inner diameter (16 mm) of the glass test tube could have significantly affected the observed $T_{ads}$. Specifically, the observations become somewhat lower than intrinsic $T_{ads}$ because the frequency of collisions with walls for traveling across the length decreases with an increase in the inner diameter. Furthermore, the other experimental conditions, i.e., tube material, gas flow, and astatine amount, differed from those in [19, 20]. Therefore, further studies in dry distillation experiments allow to determine the $T_{ads}$ of astatine owing to the fundamental chemical interest in the formation of volatile astatine species.

## Conclusions

This study obtained optimized conditions of dry distillation in a glass test tube (length, 18 cm; inner diameter, 16 mm), filled with nitrogen gas, by heating the third portion of the test tube with an electric furnace at 650 °C, which was used for the preparation of astatine solutions for the production of $^{209–211}$At in the $^{nat}$Pb($^7$Li, xn)$^{207–211}$At reaction. The heating time that was sufficient to complete the separation was ~ 10 min. Cooling of the middle portion of the test tube below the $T_{ads}$ of ~ 20 °C allowed to effectively collect astatine, which was separated from the target at high purity by dry distillation with high yield (~ 93%).

The $T_{ads}$ of astatine on glass was evaluated at ~ 20 °C and approximately − 10 °C in this study and Ref. [18], respectively. The $T_{ads}$s of ~ 20 °C and approximately − 10 °C were related to the respective concentrations of astatine on the order of ~ $10^{10}$ and ~ $10^{12}$ atoms. Owing to the the relation between $T_{ads}$s and astatine amounts used, the comparison with the observations suggested that $T_{ads}$ of approximately − 10 °C was revalidated for $At_2$, whereas $T_{ads}$ of ~ 20℃ was not for $At_2$ but for the mixture of $At_2$ and At. To determine the $T_{ads}$ and volatile chemical species of astatine, further dry-chemistry-based experiments need to be performed.

**Acknowledgments** The authors thank the crew of the JAEA Tandem Accelerator for accelerator operation. We are thankful to M. Asai for utilizing the Ge detector. This work was supported by JSPS KAKENHI Grant Number JP18K11939.

## References

1. Beyer GJ, Dreyer R, Odrich H, Rösch F (1981) Production of $^{211}$At at the Rossendorf-cyclotron U-120. Radiochem Radioanal Lett 47:63–66

2. Doberenz V, Nhan DD, Dreyer R, Milanov M, Norseyev YV, Khalkin VA (1982) Preparation of astatine of high specific activity in solutions of given composition. Radiochem Radioanal Lett 52:119–128
3. Lambrecht RM, Mirzadeh S (1985) Cyclotron isotopes and radiopharmaceuticals—XXXV Astatine-211. Int J Appl Radiat Isot 36:443–450
4. Larsen RH, Wieland BW, Zalutsky MR (1996) Evaluation of an internal cyclotron target for the production of $^{211}$At via the $^{209}$Bi(α,2n)$^{211}$At reaction. Appl Radiat Isot 47:135–143
5. Henriksen G, Messelt S, Olsen E, Larsen RH (2001) Optimisation of cyclotron production parameters for the $^{209}$Bi(α,2n)$^{211}$At reaction related to biomedical use of $^{211}$At. Appl Radiat Isot 54:839–844
6. Lindegren S, Bäck T, Jensen HJ (2001) Dry-distillation of astatine-211 from irradiated bismuth targets: a time-saving procedure with high recovery yields. Appl Radiat Isot 55:157–160
7. Hermanne A, Tárkányi F, Takács S, Szücs Z, Shubin YN, Dityuk AI (2005) Experimental study of the cross-sections of α-particle induced reactions on $^{209}$Bi. Appl Radiat Isot 63:1–9
8. Lebeda O, Jiran R, Ráliš J, Štursa J (2005) A new internal target system for production of $^{211}$At on the cyclotron U-120M. Appl Radiat Isot 63:49–53
9. Groppi F, Bonardi ML, Birattari C, Menapace E, Abbas K, Holzwarth U, Alfarano A, Morzenti S, Zona C, Alfassi ZB (2005) Optimisation study of α-cyclotron production of At-211/Po-211 g for high-LET metabolic radiotherapy purposes. Appl Radiat Isot 63:621–631
10. Morzenti S, Bonardi ML, Groppi F, Zona C, Persocp E, Menapace E, Alfassi ZB (2008) Cyclotron production of $^{211}$At/$^{211g}$Po by $^{209}$Bi(α,2n) reaction. J Radioanal Nucl Chem 276:843–847
11. Nagatsu K, Minegishi K, Fukuda M, Suzuki H, Hasegawa S, Zhang MR (2014) Production of $^{211}$At by a vertical beam irradiation method. Appl Radiat Isot 94:363–371
12. Roy K, Lahiri S (2008) Production and separation of astatine radionuclides: some new addition to astatine chemistry. Appl Radiat Isot 66:571–576
13. Maiti M, Lahiri S (2011) Production cross section of At radionuclides from $^{7}$Li + $^{nat}$Pb and $^{9}$Be + $^{nat}$Tl reactions. Phys Rev C 84:067601–067601
14. Nishinaka I, Yokoyama A, Washiyama K, Maeda E, Watanabe S, Hashimoto K, Ishioka NS, Makii H, Toyoshima A, Yamada N, Amano R (2015) Production and separation of astatine isotopes in the $^{7}$Li + $^{nat}$Pb reaction. J Radioanal Nucl Chem 304:1077–1083
15. Nishinaka I, Hashimoto K, Suzuki H (2018) Thin layer chromatography for astatine and iodine in solutions prepared by dry distillation. J Radioanal Nucl Chem 318:897–905
16. Nishinaka I, Hashimoto K, Suzuki H (2019) Speciation of astatine reacted with oxidizing and reducing reagents by thin layer chromatography: formation of volatile astatine. J Radioanal Nucl Chem 322:2003–2009
17. Wilbur DS (2013) Enigmatic astatine. Nat Chem 5:246
18. Nishinaka I, Ishioka NS, Watanabe S, Sasaki I, Azim MAU (2020) Preparation of no-carrier-added $^{211}$At solutions by a simple dry distillation method in the $^{209}$Bi($^{4}$He,2n)$^{211}$Ar reaction. J Radioanal Nucl Chem 326:743–751
19. Merinis J, Legou Y, Bouissières (1972) Etude de la formation en phase gazeuse de composes interhalogenes d'astate par thermochromatographie. Radiochem Radioanal Lett 11:59–64 (in French)
20. Serov A, Aksenov N, Bozhikov G, Eichler R, Dressler R, Lebedev V, Petrushkin O, Piguet D, Shishkin S, Tereshatov E, Türler A. Vögele A, Wittwer D, Gäggeler HW (2011) Adsorption interaction of astatine species with quartz and gold surfaces. Radiochim Acta 99:593–599